# Machine learning accelerated first-principles predictions of the stability and mechanical property of $L1_2$-strengthened Cobalt-based superalloy

Shengkun Xi [a,1], Jinxin Yu [a,1], Longke Bao [a], Liuping Chen [a], Zhou Li [a], Rongpei Shi [a***], Cuiping Wang [b**], Xingjun Liu [a, b, c*]

a. School of Materials Science and Engineering, and Institute of Materials Genome and Big Data, Harbin Institute of Technology, Shenzhen, 518055, PR China
b. College of Materials and Fujian Provincial Key Laboratory of Materials Genome, Xiamen University, Xiamen, 361005, PR China
c. State Key Laboratory of Advanced Welding and Joining, Harbin Institute of Technology, Shenzhen, 518055, PR China

Table S1 Data of Co-Al-W-X, Co-V-Ti-X and Co-V-Ir-X systems for training machine learning models.

| main #1 | main #2 | main #3 | TM | Occupancy | Structure | $C_{11}$ | $C_{12}$ | $C_{44}$ | B | G | E |
|---|---|---|---|---|---|---|---|---|---|---|---|
| Co | Al | W | Sc | Al | $L1_2$ | 323 | 182 | 176 | 229 | 122 | 311 |
| Co | Al | W | Ti | Al | $L1_2$ | 336 | 190 | 183 | 239 | 126 | 323 |
| Co | Al | W | V | Al | $L1_2$ | 360 | 184 | 188 | 243 | 139 | 349 |
| Co | Al | W | Cr | Al | $L1_2$ | 373 | 182 | 192 | 245 | 145 | 364 |
| Co | Al | W | Mn | Al | $L1_2$ | 358 | 175 | 182 | 234 | 138 | 345 |
| Co | Al | W | Fe | Co | $D0_{19}$ | - | - | - | - | - | - |
| Co | Al | W | Ni | Co | $L1_2$ | 294 | 174 | 171 | 214 | 113 | 287 |

* Correspondance to: Xingjun Liu.
** Correspondance to: Cuiping Wang.
*** Correspondance to: Rongpei Shi.
[1] Shengkun Xi and Jinxin Yu contributed equally to this work.
E-mail address : xjliu@hit.edu.cn (Xingjun Liu), wangcp@xmu.edu.cn (Cuiping Wang), shirongpei@hit.edu.cn (Rongpei Shi)

| | | | | | | | | | | | |
|---|---|---|---|---|---|---|---|---|---|---|---|
| Co | Al | W | Y | Al | $D0_{19}$ | - | - | - | - | - | - |
| Co | Al | W | Zr | Al | $L1_2$ | 331 | 183 | 178 | 232 | 125 | 318 |
| Co | Al | W | Nb | Al | $L1_2$ | 360 | 183 | 186 | 242 | 138 | 348 |
| Co | Al | W | Mo | Al | $L1_2$ | 372 | 181 | 186 | 245 | 142 | 358 |
| Co | Al | W | Tc | Al | $L1_2$ | 377 | 179 | 189 | 245 | 145 | 364 |
| Co | Al | W | Ru | Co | $D0_{19}$ | - | - | - | - | - | - |
| Co | Al | W | Rh | Co | $L1_2$ | 305 | 189 | 176 | 227 | 113 | 291 |
| Co | Al | W | Pd | Co | $D0_{19}$ | - | - | - | - | - | - |
| Co | Al | W | Hf | Al | $L1_2$ | 333 | 187 | 178 | 235 | 124 | 317 |
| Co | Al | W | Ta | Al | $L1_2$ | 369 | 190 | 187 | 250 | 139 | 352 |
| Co | Al | W | Re | Al | $L1_2$ | 383 | 184 | 192 | 250 | 147 | 369 |
| Co | Al | W | Os | Al | $L1_2$ | 378 | 179 | 189 | 245 | 146 | 366 |
| Co | Al | W | Ir | Co | $L1_2$ | 318 | 197 | 178 | 237 | 116 | 299 |
| Co | Al | W | Pt | Co | $L1_2$ | 307 | 192 | 177 | 230 | 113 | 291 |
| Co | V | Ti | Cr | Ti | $L1_2$ | 364 | 175 | 184 | 238 | 141 | 353 |
| Co | V | Ti | Ir | Co | $L1_2$ | 344 | 176 | 175 | 232 | 130 | 329 |
| Co | V | Ti | Mo | Ti | $L1_2$ | 363 | 174 | 181 | 237 | 139 | 350 |
| Co | V | Ti | Nb | Ti | $L1_2$ | 350 | 174 | 174 | 233 | 132 | 334 |
| Co | V | Ti | Ni | Co | $L1_2$ | 343 | 172 | 172 | 229 | 130 | 328 |
| Co | V | Ti | Os | Co | $L1_2$ | 345 | 179 | 170 | 234 | 127 | 324 |
| Co | V | Ti | Re | Ti | $L1_2$ | 382 | 191 | 184 | 254 | 141 | 358 |
| Co | V | Ti | Ru | Co | $L1_2$ | 335 | 177 | 170 | 230 | 125 | 318 |
| Co | V | Ti | Ta | Ti | $L1_2$ | 351 | 176 | 175 | 234 | 132 | 335 |
| Co | V | Ti | W | Ti | $L1_2$ | 366 | 177 | 183 | 240 | 140 | 352 |
| Co | V | Ti | Fe | Co | $L1_2$ | 337 | 171 | 171 | 226 | 128 | 323 |
| Co | V | Ti | Hf | Ti | $L1_2$ | 336 | 170 | 166 | 226 | 125 | 318 |
| Co | V | Ti | Mn | Co | $L1_2$ | 326 | 168 | 166 | 221 | 123 | 311 |
| Co | V | Ti | Pd | Co | $L1_2$ | 335 | 171 | 169 | 226 | 126 | 320 |

| | | | | | | | | | | | |
|---|---|---|---|---|---|---|---|---|---|---|---|
| Co | V | Ti | Pt | Co | $L1_2$ | 344 | 173 | 173 | 230 | 130 | 330 |
| Co | V | Ti | Rh | Co | $L1_2$ | 341 | 175 | 173 | 230 | 129 | 326 |
| Co | V | Ti | Sc | Ti | $L1_2$ | 312 | 171 | 164 | 218 | 116 | 297 |
| Co | V | Ti | Tc | Ti | $L1_2$ | 368 | 175 | 185 | 240 | 142 | 356 |
| Co | V | Ti | Y | Ti | $L1_2$ | 286 | 159 | 150 | 201 | 105 | 270 |
| Co | V | Ti | Zr | Ti | $L1_2$ | 332 | 166 | 163 | 222 | 124 | 315 |
| Co | V | Ir | Sc | V | $D0_{19}$ | - | - | - | - | - | - |
| Co | V | Ir | Ti | Co | $D0_{19}$ | - | - | - | - | - | - |
| Co | V | Ir | Cr | Co | $D0_{19}$ | - | - | - | - | - | - |
| Co | V | Ir | Mn | Co | $D0_{19}$ | - | - | - | - | - | - |
| Co | V | Ir | Fe | Co | $D0_{19}$ | - | - | - | - | - | - |
| Co | V | Ir | Ni | Co | $D0_{19}$ | - | - | - | - | - | - |
| Co | V | Ir | Y | V | $D0_{19}$ | - | - | - | - | - | - |
| Co | V | Ir | Zr | V | $D0_{19}$ | - | - | - | - | - | - |
| Co | V | Ir | Nb | Co | $D0_{19}$ | - | - | - | - | - | - |
| Co | V | Ir | Mo | Co | $D0_{19}$ | - | - | - | - | - | - |
| Co | V | Ir | Tc | Co | $D0_{19}$ | - | - | - | - | - | - |
| Co | V | Ir | Ru | Co | $D0_{19}$ | - | - | - | - | - | - |
| Co | V | Ir | Rh | Co | $D0_{19}$ | - | - | - | - | - | - |
| Co | V | Ir | Pd | Co | $D0_{19}$ | - | - | - | - | - | - |
| Co | V | Ir | Hf | V | $D0_{19}$ | - | - | - | - | - | - |
| Co | V | Ir | Ta | Co | $D0_{19}$ | - | - | - | - | - | - |
| Co | V | Ir | W | Co | $D0_{19}$ | - | - | - | - | - | - |
| Co | V | Ir | Re | Ir | $D0_{19}$ | - | - | - | - | - | - |
| Co | V | Ir | Os | Co | $D0_{19}$ | - | - | - | - | - | - |
| Co | V | Ir | Pt | Co | $D0_{19}$ | - | - | - | - | - | - |

For the mechanical properties of $D0_{19}$ structure is more stable than $L1_2$ structure.

the mechanical properties of $L1_2$ phase are meaningless.

Table S2 Parameters of machine learning models

| Models | n_estimators | max_depth | max_features |
|---|---|---|---|
| Occupied sites prediction model | 150 | 5 | 8 |
| Stability prediction model | 100 | 9 | 1 |
| $C_{11}$ prediction model | 200 | 7 | 4 |
| $C_{12}$ prediction model | 200 | 6 | 7 |
| $C_{44}$ prediction model | 200 | 4 | 6 |
| Bulk modulus prediction model | 250 | 7 | 4 |
| Shear modulus prediction model | 250 | 5 | 8 |
| Elastic modulus prediction model | 250 | 6 | 5 |

Table S3 Correspondence between full name of features and codes

| Feature full name | Doping element | Main Element #2 | Main Element #3 |
|---|---|---|---|
| Melting Point | 1A | 2A | 3A |
| Boiling Point | 1B | 2B | 3B |
| Density | 1C | 2C | 3C |
| Relative Atomic Mass | 1D | 2D | 3D |
| Atomic Radius, Non-bonded | 1E | 2E | 3E |
| Covalent Radius | 1F | 2F | 3F |
| Electronegativity | 1G | 2G | 3G |
| 1st Ionization Energy | 1H | 2H | 3H |
| Occupied Position | 1J | - | - |

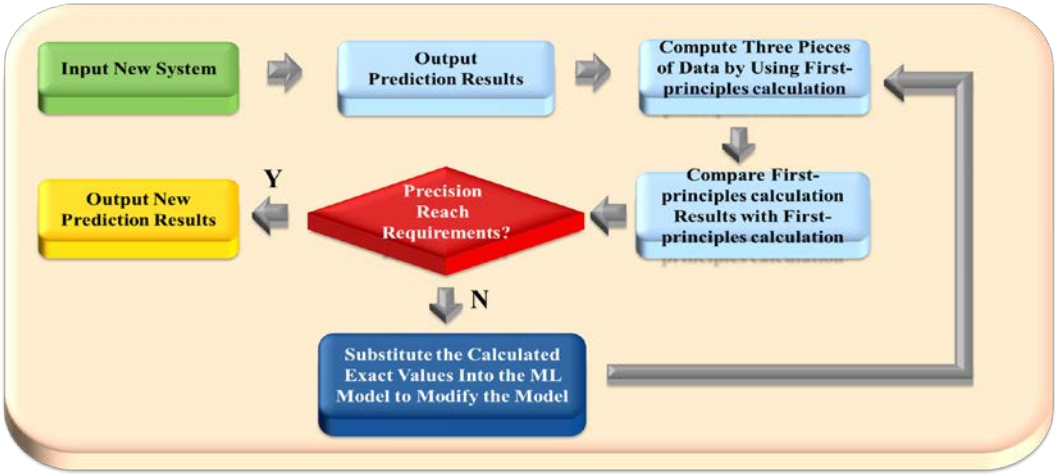


Fig. S1 Schematic illustration of the interaction between ML model and first-principles calculations for iteratively improving ML model performance.

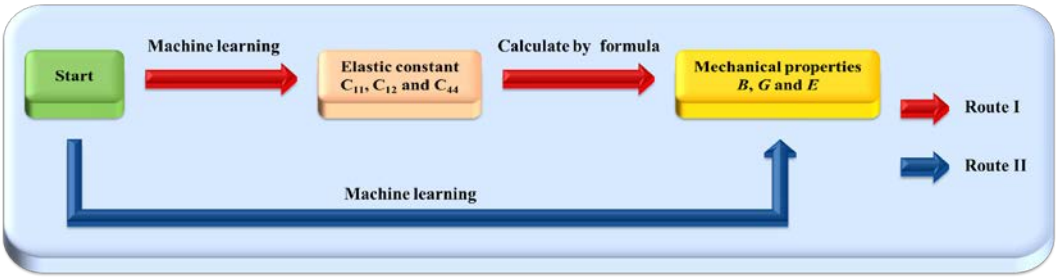


Fig. S2 Two routes for predicting mechanical properties of $L1_2$ phase. Route **I** sets $C_{11}$, $C_{12}$ and $C_{44}$ as $Y$, and calculates the mechanical properties including ***B***, ***G***, ***E*** according the formulars; Route **II** computes mechanical properties including ***B***, ***G***, ***E*** directly.

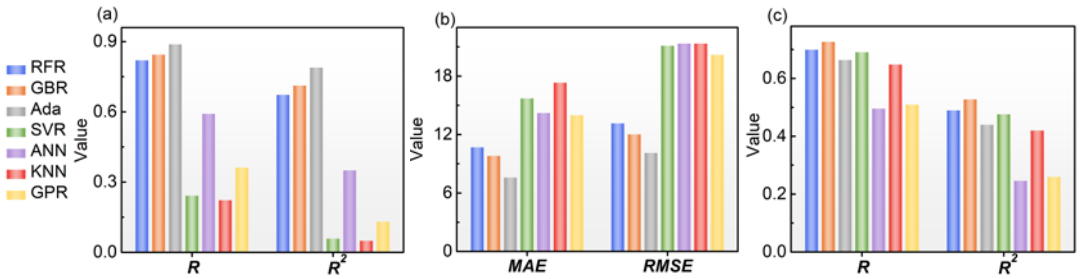

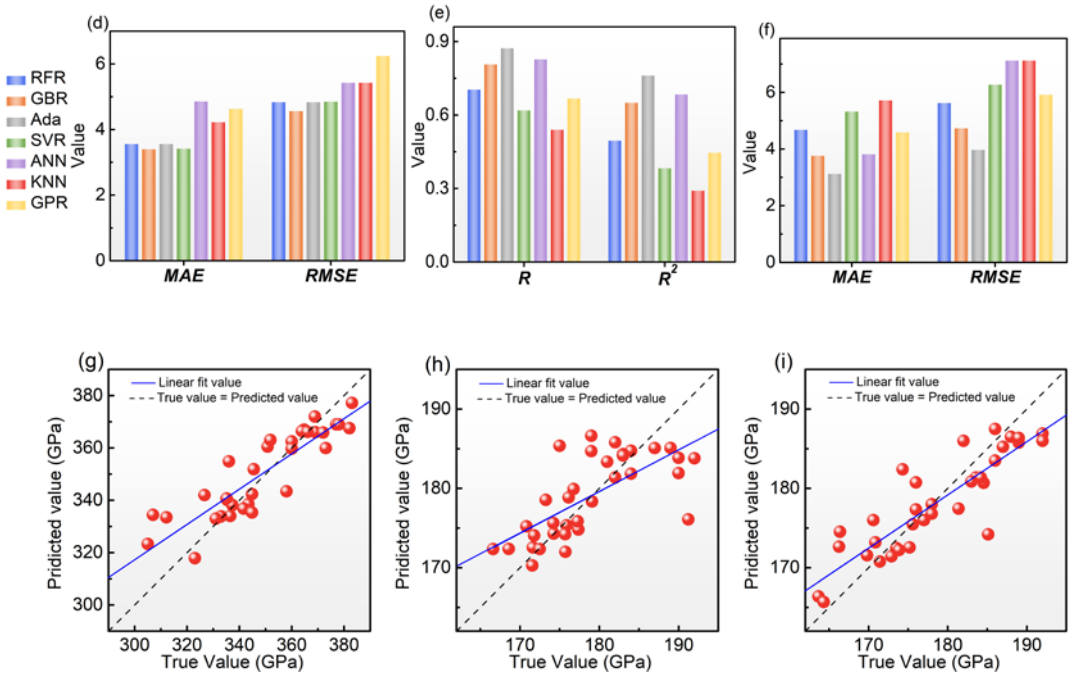


Fig. S3 The model performance of each regression model in terms of the $R$、$R^2$、*MAE* and *RMSE* on the training set by 10-fold cross-validation (Route **I**). (a) $R$, $R^2$ and (b) *MAE*, *RMSE* of $C_{11}$, (c) $R$, $R^2$ and (d) *MAE*, *RMSE* of $C_{12}$, (e) $R$, $R^2$ and (f) *MAE*, *RMSE* of $C_{44}$.; Predictions on the mechanical properties of $L1_2$ phase in Co-based superalloys based on AdaBoost Regression model (Route **I**). The X axis represents the true value, and the Y axis represents the predicted value. When the true value is equal to the predicted value, the data will be distributed on a dashedline that passes through the origin, and the slope of the dashed line is 1. (g) $C_{11}$, (h) $C_{12}$, (i) $C_{44}$

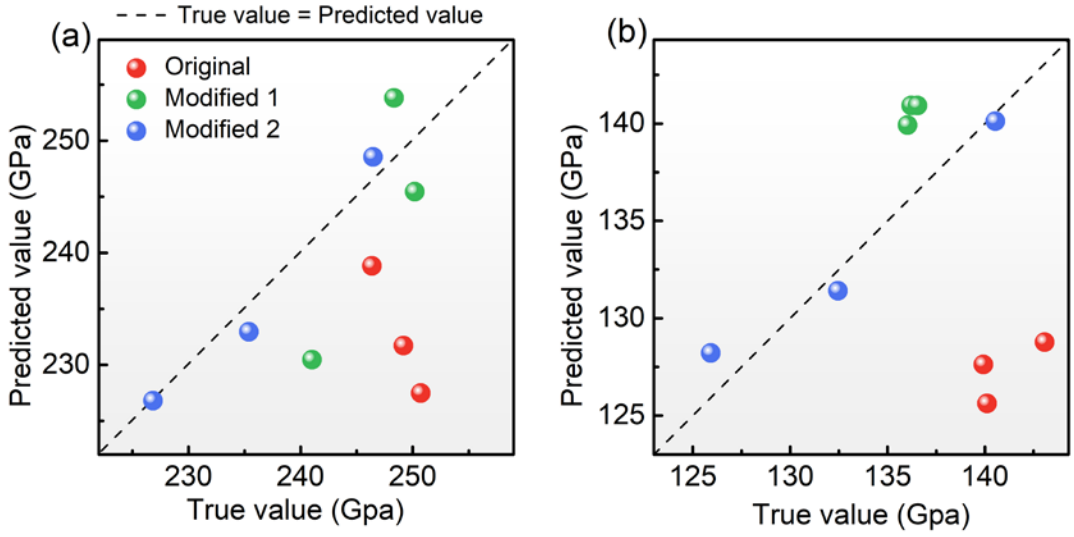

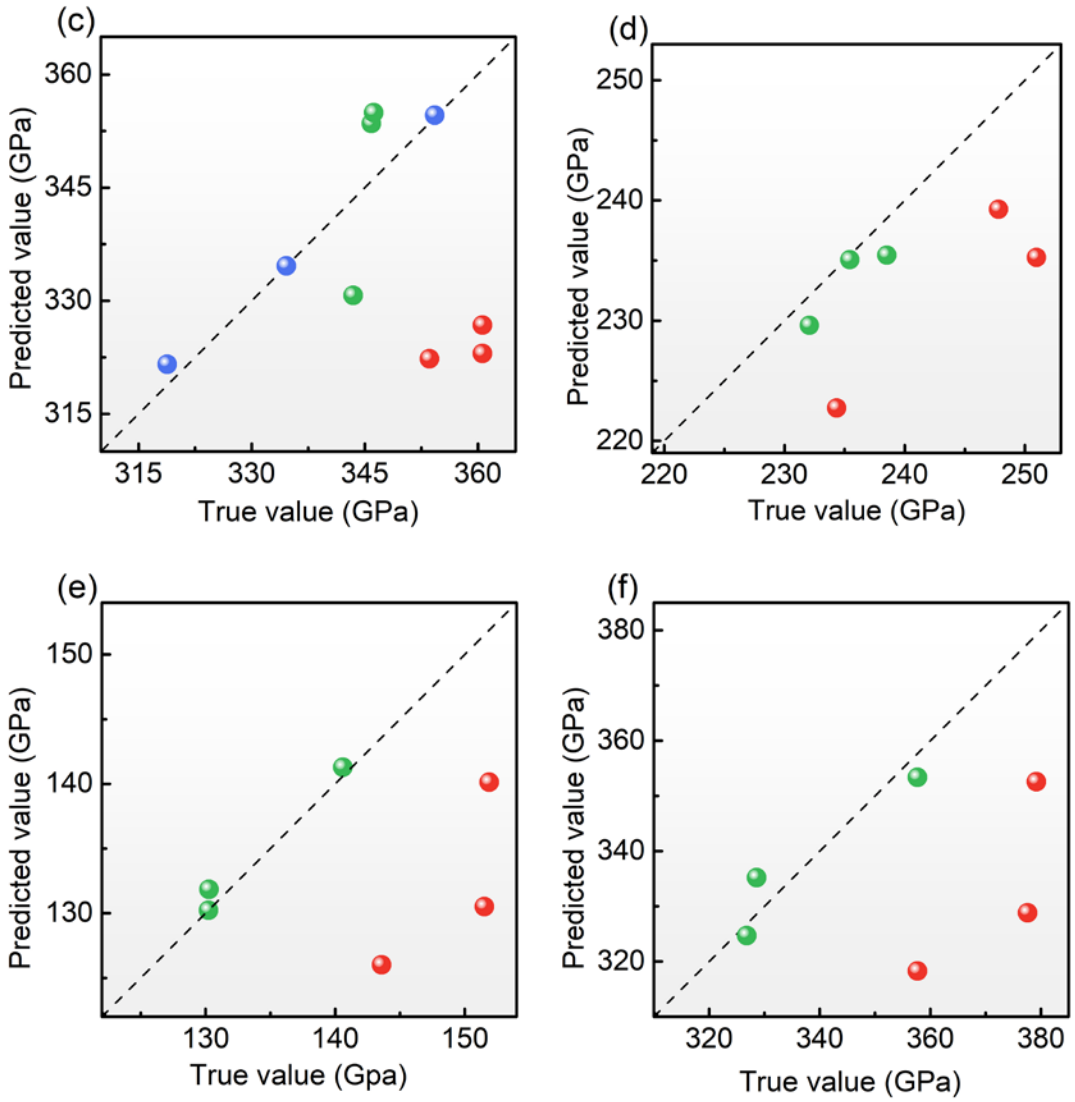


Fig. S4 The optimization process of the mechanical property prediction models of $L1_2$ phase. The red, green and blue data points represent the prediction results of the machine learning model without modified, modified once, modified twice, respectively. The results should be compared with first-principles calculations. (a) ***B***, (b) ***G***, and (c) ***E*** of Co-V-Ta-based system; (d) ***B***, (e) ***G***, and (f) ***E*** of Co-Al-V-based system

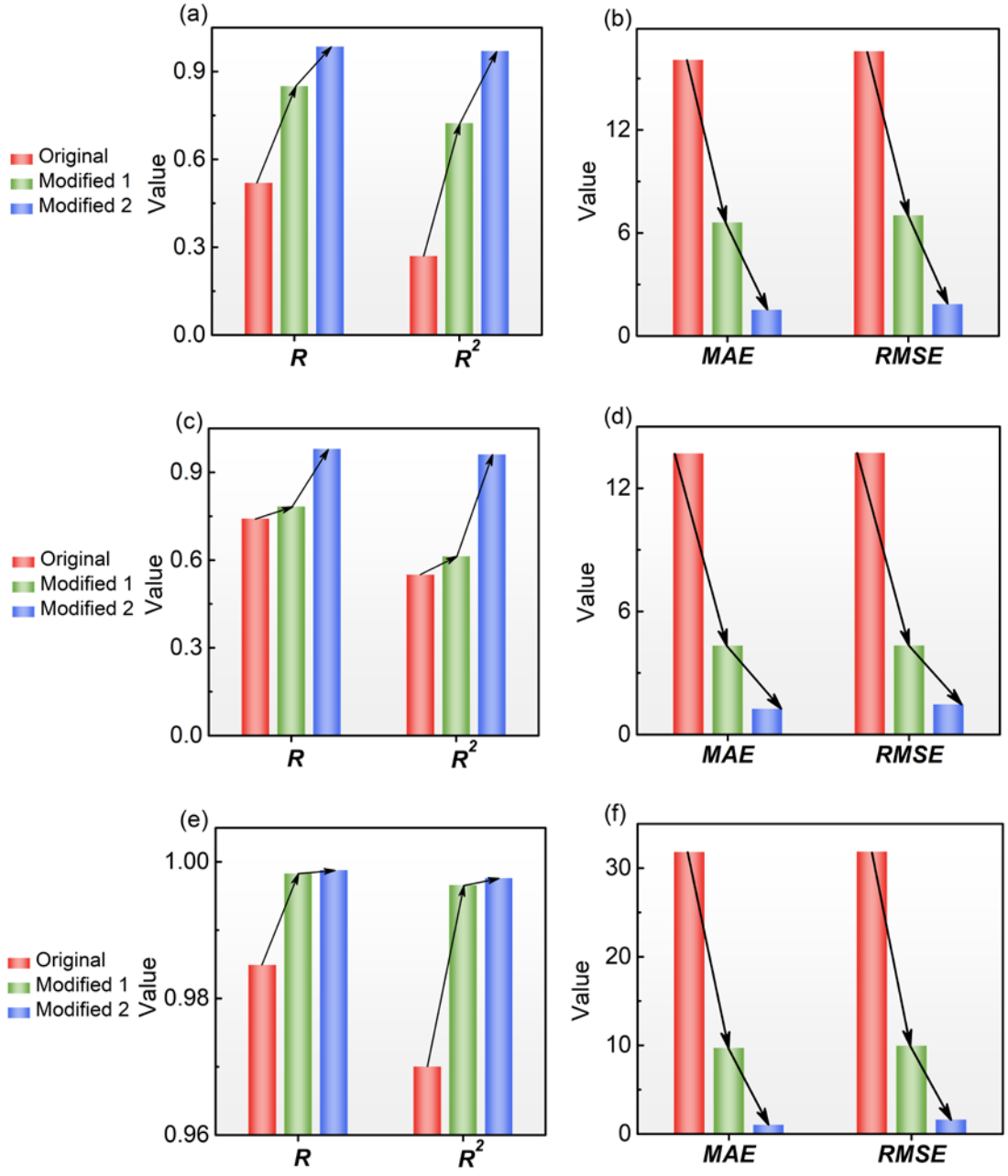


Fig. S5 The optimization process of model performance of mechanical properties prediction model of $L1_2$ phase in Co-V-Ta-based system. The red, green and blue bars represent the prediction results of the machine learning model without modified, modified once, modified twice, respectively. (a) *R* and $R^2$ and (b) *MAE* and *RMSE* of Bulk modulus (***B***), (c) *R* and $R^2$ and (d) *MAE* and *RMSE* of Shear modulus (***G***), (e) *R* and $R^2$ and (f) *MAE* and *RMSE* of Young's modulus (***E***)

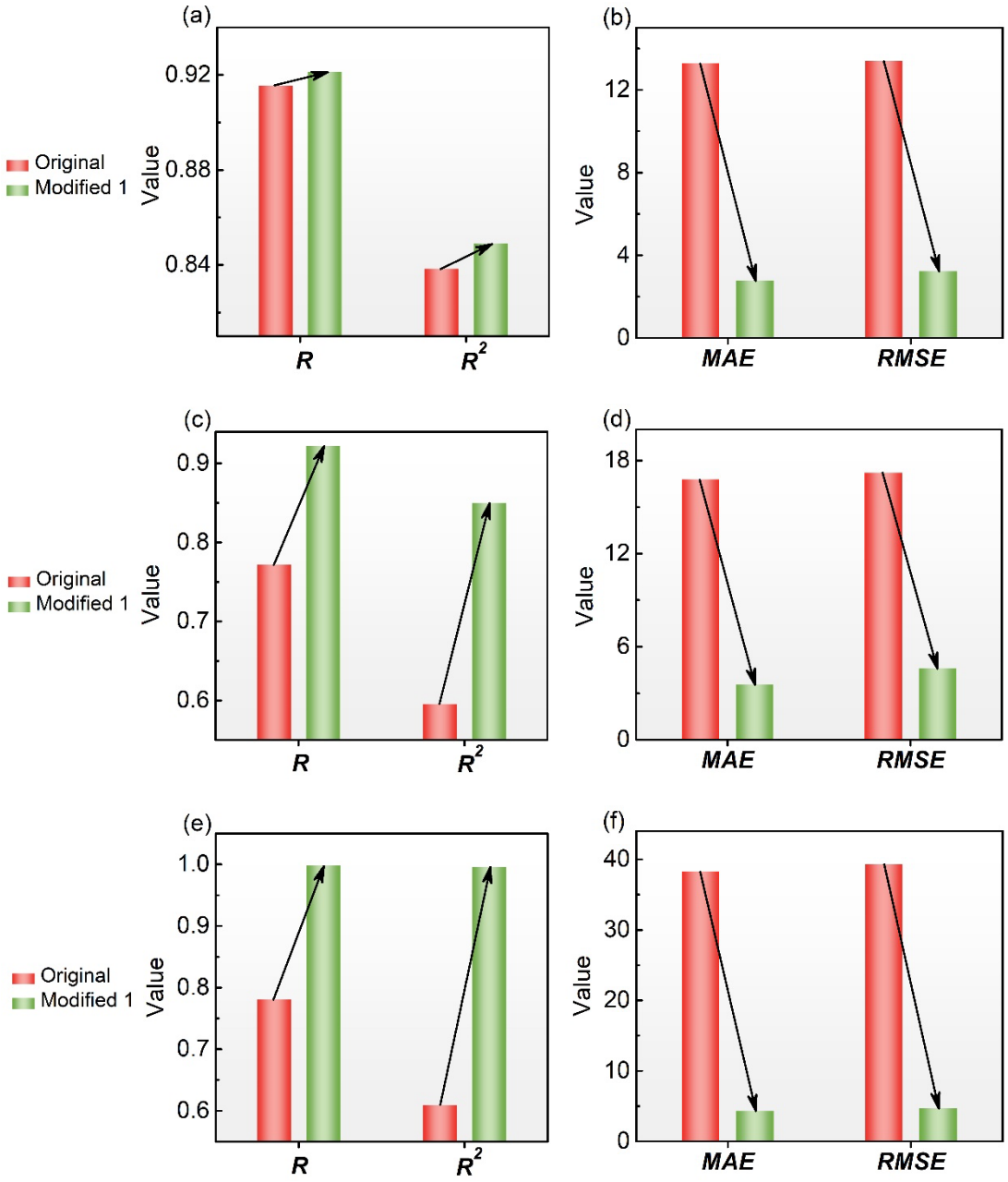


Fig. S6 The improvement process of model performance of mechanical properties prediction model of $L1_2$ phase in Co-Al-V-based system. The red and green bars represent the prediction results of the machine learning model without modified and modified once, respectively. The results should be compared with first-principles calculations. (a) *R* and $R^2$ and (b) *MAE* and *RMSE* of Bulk modulus (***B***), (c) *R* and $R^2$ and (d) *MAE* and *RMSE* of Shear modulus (***G***), (e) *R* and $R^2$ and (f) *MAE* and *RMSE* of Young's modulus (***E***)

**Calculation methods**

The elastic constant ($C$) can be written in the form of a 6 × 6 matrix:

$$\sigma_i = \sum_j C_{ij} \times \varepsilon_j = \begin{pmatrix} \sigma_1 \\ \sigma_2 \\ \sigma_3 \\ \sigma_4 \\ \sigma_5 \\ \sigma_6 \end{pmatrix} = \begin{pmatrix} C_{11} & C_{12} & C_{13} & C_{14} & C_{15} & C_{16} \\ C_{21} & C_{22} & C_{23} & C_{24} & C_{25} & C_{26} \\ C_{31} & C_{32} & C_{33} & C_{34} & C_{35} & C_{36} \\ C_{41} & C_{42} & C_{43} & C_{44} & C_{45} & C_{46} \\ C_{51} & C_{52} & C_{53} & C_{54} & C_{55} & C_{56} \\ C_{61} & C_{62} & C_{63} & C_{64} & C_{65} & C_{66} \end{pmatrix} \times \begin{pmatrix} \varepsilon_1 \\ \varepsilon_2 \\ \varepsilon_3 \\ \varepsilon_4 \\ \varepsilon_5 \\ \varepsilon_6 \end{pmatrix}, \quad (4)$$

where $\sigma_i$, $\varepsilon_i$ and $C_{ij}$ donate the stress, strain and elastic constants, respectively. The strain characterized by the tensor $\varepsilon = (\varepsilon_1, \varepsilon_2, \varepsilon_3, \varepsilon_4, \varepsilon_5, \varepsilon_6)$ is applied on the supercell to produce an infinitesimal deformation. The stress is defined as the first derivative of the total elastic strain energy with respect to the corresponding strain. The stress tensors $\sigma = (\sigma_1, \sigma_2, \sigma_3, \sigma_4, \sigma_5, \sigma_6)$ will be generated after the crystal structure is deformed by the strain ε.

Because of the cubic symmetry, only three independent elastic constants $\bar{C}_{11}$, $\bar{C}_{12}$ and $\bar{C}_{44}$ are required to describe the elastic constants. The $\bar{C}_{11}$, $\bar{C}_{12}$ and $\bar{C}_{44}$ can be calculated as follows[1]:

$$\bar{C}_{11} = (C_{11} + C_{22} + C_{33})/3 \qquad \bar{S}_{11} = (S_{11} + S_{22} + S_{33})/3, \quad (5)$$

$$\bar{C}_{12} = (C_{12} + C_{13} + C_{23})/3 \qquad \bar{S}_{12} = (S_{12} + S_{13} + S_{23})/3, \quad (6)$$

$$\bar{C}_{44} = (C_{44} + C_{55} + C_{66})/3 \qquad \bar{S}_{44} = (S_{44} + S_{55} + S_{66})/3, \quad (7)$$

where$\bar{S}_{ij}$is flexible constant matrix. The $\bar{S}_{ij}$ can be obtained by inverting the elastic constant matrix $\bar{C}_{ij}$.

The elastic properties of the $L1_2$ phase are characterized via the Voigt-Reuss-Hill (VRH) approximation as follows[2]-[4]:

$$B_v = (\bar{C}_{11} + 2\bar{C}_{12})/3 \qquad B_R = 1/(3\bar{S}_{11} + 6\bar{S}_{12}), \quad (8)$$

$$G_v = (\bar{C}_{11} - \bar{C}_{12} + 3\bar{C}_{44})/5 \qquad G_R = 5/(4\bar{S}_{11} - 4\bar{S}_{12} + 3\bar{S}_{44}), \quad (9)$$

$$E_v = (9B_vG_v)/(3B_v + G_v) \qquad E_R = (9B_RG_R)/(3B_R + G_R), \quad (10)$$

$$B = (B_v + B_R)/2, \quad (11)$$

$$G = (G_v + G_R)/2, \quad (12)$$

$$E = (E_v + E_R)/2, \quad (13)$$

**Reference**

[1] Xi S, Chen L, Bao L, Han J, Yu J, Li Z, Xu W, Deng B, Wang C, Liu X. Effects

of alloying elements on the atomic structure, elastic and thermodynamic properties of $L1_2$-$Co_3$(V, Ti) compound. Materials Today Communications 2022; 102931.

[2] Chung D. Elastic moduli of single crystal and polycrystalline MgO. Philosophical Magazine 1963;8: 833-841.

[3] Anderson O. A simplified method for calculating the Debye temperature from elastic constants. Journal of Physics and Chemistry of Solids 1963; 24: 909-917.

[4] Chung D, Buessem W. The Voigt - Reuss - Hill (VRH) approximation and the elastic moduli of polycrystalline ZnO, $TiO_2$ (Rutile), and α - $Al_2O_3$. Journal of applied physics 1968; 39(6): 2777-2782.